

# Reconstructing the global dynamics of under-ascertained COVID-19 cases and infections

*Authors: Timothy W. Russell<sup>1\*</sup>, Nick Golding<sup>2</sup>, Joel Hellewell<sup>1</sup>, Sam Abbott<sup>1</sup>, Carl A B Pearson<sup>1</sup>, Kevin van Zandvoort<sup>1</sup>, Christopher I Jarvis<sup>1</sup>, Hamish Gibbs<sup>1</sup>, Yang Liu<sup>1</sup>, Rosalind M. Eggo<sup>1</sup>, W. John Edmunds<sup>1</sup>, Adam J. Kucharski<sup>1</sup> on behalf of the CMMID COVID-19 working group*

<sup>1</sup>*Centre for Mathematical Modelling of Infectious Diseases, London School of Hygiene & Tropical Medicine*

<sup>2</sup>*Telethon Kids Institute and Curtin University, Perth, Western Australia*

*\* Corresponding author: [timothy.russell@lshtm.ac.uk](mailto:timothy.russell@lshtm.ac.uk)*

*CMMID COVID-19 working group members (order selected at random): Arminster K Deol, C Julian Villabona-Arenas, Thibaut Jombart, Carl A B Pearson, Kathleen O'Reilly, James D Munday, Sophie R Meakin, Rachel Lowe, Amy Gimma, Akira Endo, Emily S Nightingale, Graham Medley, Anna M Foss, Gwenan M Knight, Kiesha Prem, Stéphane Hué, Charlie Diamond, James W Rudge, Katherine E. Atkins, Megan Auzenberg, Stefan Flasche, Rein M G J Houben, Billy J Quilty, Petra Klepac, Matthew Quaife, Sebastian Funk, Quentin J Leclerc, Jon C Emery, Mark Jit, David Simons, Nikos I Bosse, Simon R Procter, Fiona Yueqian Sun, Samuel Clifford, Katharine Sherratt, Alicia Rosello, Nicholas G. Davies, Oliver Brady, Damien C Tully, Georgia R Gore-Langton.*

## **Abstract**

**Background:** Asymptomatic or subclinical SARS-CoV-2 infections are often unreported, which means that confirmed case counts may not accurately reflect underlying epidemic dynamics. Understanding the level of ascertainment (the ratio of confirmed symptomatic cases to the true number of symptomatic individuals) and undetected epidemic progression is crucial to informing COVID-19 response planning, including the introduction and relaxation of control measures. Estimating case ascertainment over time allows for accurate estimates of specific outcomes such as seroprevalence, which is essential for planning control measures.

**Methods:** Using reported data on COVID-19 cases and fatalities globally, we estimated the proportion of symptomatic cases (i.e. any person with any of fever  $\geq 37.5^{\circ}\text{C}$ , cough, shortness of breath, sudden onset of anosmia, ageusia or dysgeusia illness) that were reported in 210 countries and territories, given those countries had experienced more than ten deaths. We used published estimates of the baseline case fatality ratio (CFR), which was adjusted for delays and under-ascertainment, then calculated the ratio of this baseline CFR to an estimated local delay-adjusted CFR to estimate the level of under-ascertainment in a particular location. We then fit a Bayesian Gaussian process model to estimate the temporal pattern of under-ascertainment.

**Results:** We estimate that, during March 2020, the median percentage of symptomatic cases detected across the 84 countries which experienced more than ten deaths ranged from 2.38% (Bangladesh) to 99.6% (Chile). Across the ten countries with the highest number of total confirmed cases as of 6th July 2020, we estimated that the peak number of symptomatic cases ranged from 1.4 times (Chile) to 17.8 times (France) larger than reported. Comparing our model with national and regional seroprevalence data where available, we find that our estimates are consistent with observed values. Finally, we estimated seroprevalence for each country. Despite low case detection in some countries, our results that adjust for this still suggest that all countries have had only a small fraction of their populations infected as of July 2020.

**Conclusions:** We found substantial under-ascertainment of symptomatic cases, particularly at the peak of the first wave of the SARS-CoV-2 pandemic, in many countries. Reported case counts will therefore likely underestimate the rate of outbreak growth initially and underestimate the decline in the later stages of an epidemic. Although there was considerable under-reporting in many locations, our estimates were consistent with emerging serological data, suggesting that the proportion of each country's population infected with SARS-CoV-2 worldwide is generally low.

**Funding:** Wellcome Trust, Bill & Melinda Gates Foundation, DFID, NIHR, GCRF, ARC.

**Key words:** Case ascertainment, COVID-19, SARS-CoV-2, surveillance, under-reporting, situational awareness, outbreak analysis

## **Introduction**

The pandemic of the novel coronavirus SARS-CoV-2 has caused 11.7 million confirmed cases and 538,818 deaths as of 6<sup>th</sup> July 2020 (1). As a precautionary measure, or in response to locally detected outbreaks, countries have introduced control measures with varying degrees of stringency (1), including isolation and quarantine; school and workplace closures; bans on social gatherings; physical distancing and face coverings; and stay-at-home orders (2,3). Several features of SARS-CoV-2 make accurate detection during an ongoing epidemic challenging (4–6), including high transmissibility (3,7–9); an incubation period with a long-tailed distribution (10); pre-symptomatic transmission (11); and the existence of asymptomatic infections, which may also contribute to transmission (12). These attributes mean that infections can go undetected (13) and that countries may only detect and report a fraction of their infections (3,14).

Understanding the extent of unreported infections in a given country is crucial for situational awareness. If the true size of the epidemic can be estimated, this enables a more reliable assessment of how and when non-pharmaceutical interventions (NPIs) should be both introduced, as infections rise, or relaxed as infections fall (3). Estimates of infection prevalence are also important for obtaining accurate measures of transmission: if the proportion of infections reported declines as the epidemic rises, the number of confirmed cases will grow slower than the actual underlying epidemic. Likewise, if detection rises as the epidemic declines, it may appear that transmission is not declining as fast as it is in reality. Underdetection of cases also makes it challenging to estimate at what stage of the epidemic a particular country is (15): viewed in isolation, case incidence data could reflect a very large undetected epidemic, or a smaller, better reported epidemic.

To estimate how the levels of under-ascertainment vary over time, we present a modelling framework that combines data on reported cases and deaths, and published severity estimates. We apply our methods to countries that have reported more than ten deaths to date, then use these under-ascertainment estimates to reconstruct global epidemics in all countries where case and death time series data are available. We also compare the model estimates for cumulative incidence against existing seroprevalence results. Finally, we present the adjusted case curves for the ten countries with the highest confirmed and adjusted case numbers, as well as global prevalence estimates for SARS-CoV-2.

## **Methods**

As SARS-CoV-2 infections that generate mild symptoms are more likely to be missed than severe cases, the ratio of cases to deaths, adjusting for delays from report to fatal outcome, can provide information on the possible extent of undetected symptomatic infections. Using a Bayesian Gaussian process model, we estimate changes in under-ascertainment over time, as described below.

### **Adjusting for delay from confirmation to death**

In real time, simply dividing deaths to date by cases to date leads to a biased estimate of the case fatality ratio (CFR), because this naive calculation does not account for delays from confirmation of a case to death, and under-ascertainment of cases (5,6) and in some circumstances, under-ascertainment of deaths too. Using the distribution of the delay from hospitalisation to death for cases that are fatal, we can estimate how many cases so far are expected to have known outcomes (i.e. death or recovery),

and hence adjust the naive estimates of CFR to account for these delays and produce a delay-adjusted CFR (dCFR). Separately published dCFR estimates for a given country can be used to estimate the number of symptomatic cases that would be expected for a given dCFR trajectory. Available estimates for the CFR that adjust for under-reporting typically range from 1–1.7% (7–10). Large studies in China and South Korea estimate the CFR at 1.38% (95% CrI: 1.23–1.53%) (9) and 1.7% (95% CrI: 1.1–2.5%) (7) respectively.

### **Inferring level of under-ascertainment**

Assuming a baseline CFR of 1.4% (95% CrI: 1.2% - 1.5%), the ratio of this baseline CFR to our estimate of the dCFR for a given country can be used to derive a crude estimate of the proportion of symptomatic cases that go unreported for this country. For each country we calculate the dCFR on each day and use the ratio of the baseline CFR to the dCFR estimate to produce daily estimates of the proportion of unreported cases. We then use a Gaussian process (GP) model to fit a time-dependent under-ascertainment rate for each country. A more detailed description of the methods, including the mathematical details of the Gaussian process and the different sources of uncertainty present in the model, can be found in the Supplementary Material.

With the aim of developing a parsimonious and easily transferable analysis framework, we assume the same baseline CFR for all countries in the main results. Given that CFR varies substantially with age (5), this induces a certain amount of error in our estimates, especially for countries with age distributions significantly different to China, where the data used to derive the baseline CFR estimates originated (5). Therefore, we include a version of all the main results where we compute an indirectly adjusted baseline CFR, using the underlying age distribution of each country using the `wpp2019` R package (16) and the age-stratified CFR estimates from (17) in the supplementary material (Figures S5, S6 and S7), where we also include a verbose limitations section discussing at length the potential errors induced under such assumptions.

### **Relationship between under-ascertainment and testing**

We attempt to characterise the relationship between testing and case ascertainment using our temporal under-ascertainment estimates and testing data for many countries from OurWorldInData (18). We do so by performing a correlation test between the two for all countries we had both data for. The resulting bivariate scatterplot is included in the supplementary material (Figure S3).

### **Comparison against seroprevalence estimates**

We attempted to reconstruct the infection curves by first adjusting the reported case data for under-ascertainment (Figure 1). We then adjust further these estimated symptomatic case curves so that they represent all infections. We do so using the assumption that 50% of infections are asymptomatic overall, with an assumed wide range between 10% - 70% and mean-lagging the time point to adjust for the delay between onset of symptoms to confirmation (19).

### **Data and code availability**

The data we use is publicly available online from the European Centre for Disease Control (ECDC) (20). The code for the dCFR and under-reporting estimation model can be found here: [https://github.com/thimotei/CFR\\_calculation](https://github.com/thimotei/CFR_calculation). The code to read in the under-ascertainment data and to reproduce the figures in this analysis can be found here: [https://github.com/thimotei/covid\\_underreporting](https://github.com/thimotei/covid_underreporting).

## **Results**

We estimated substantial variation in the proportion of symptomatic cases detected over time in many of the countries considered (Figure 1 & Figure S1). For example, during March the median percentage of symptomatic cases detected across the 84 countries which experienced more than ten deaths ranged from 2.38% (Bangladesh) to 99.6% (Chile). Also during March, the median percentage of symptomatic cases detected across Europe ranged from 4.81% (France) to 85.5% (Cyprus).

Countries might expect to detect an increasing proportion of symptomatic cases if they scale up testing effort in response to the outbreak. To measure this, we compared our estimates for the proportion of cases detected with the number of tests performed per new case each day, which can provide an indication of testing effort with a country (18). Taking a moving average with a 7-day window, we found that countries that showed high testing effort did not necessarily have high levels of case ascertainment. For example, in a two-week period in March the United Kingdom performed 80 tests per new case (the mean across Europe during the same period was 27 tests per new case). However, we estimate that also in the UK only between 3-10% of symptomatic cases were being detected (Figure 1). Overall, we found a weak positive correlation between testing effort and case ascertainment (Kendall's correlation coefficient of 0.16). This suggests that increased testing effort can help to improve case ascertainment, but on its own is not enough to guarantee low levels of under-ascertainment.

Using our temporal under-ascertainment trends, we estimate that during March, April, and May the percentage of symptomatic cases detected in European countries and averaged over time ranged from 4.8% - 86% (France - Cyprus), 5.8% - 100% (France - Belarus) and 11% - 86% (Hungary - Cyprus) respectively. By comparison, the number of reported tests performed per new confirmed case, averaged over the month in question, ranged between 2.7 to 76 in March (Belgium - Portugal), 2.7 to 832 in April (Belgium - Slovakia) and 12 to 1334 (Ukraine - Lithuania) in May.

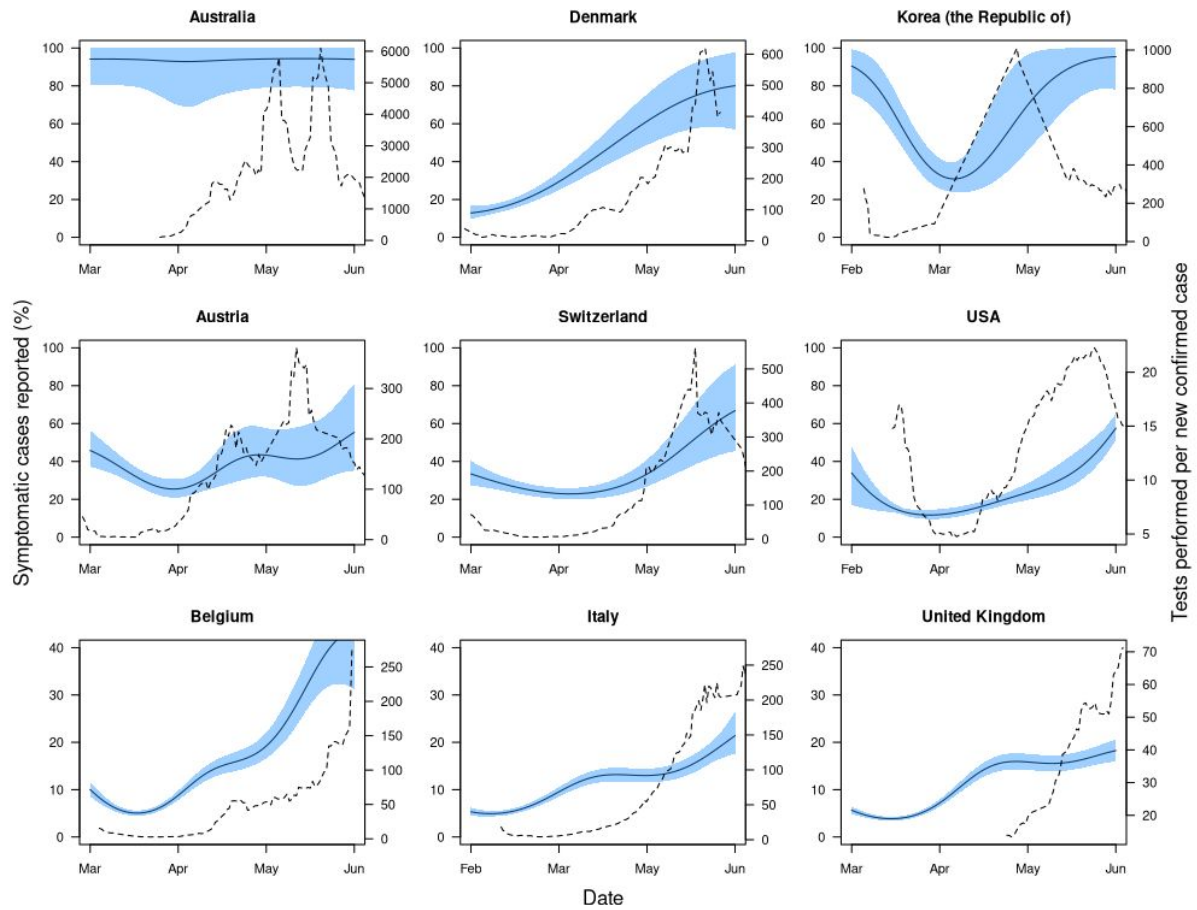


**Figure 1: Illustrative examples of temporal variation in under-ascertainment and testing effort.** Nine countries under-ascertainment and testing effort dynamics, where the under-ascertainment dynamics display a typical U-trend. The solid black line is the estimated median proportion of symptomatic cases ascertained over time and the shaded blue region is the 95% credible interval of these ascertainment estimates. Dashed line shows the reported testing effort, which we defined as a 7-day moving average of the number of new tests per new case reported each day.

Adjusting confirmed case data for under-ascertainment to obtain estimated symptomatic case curves, we found a much larger and more peaked epidemic in the ten countries with the highest total number of confirmed cases and the ten with the highest number of adjusted cases as of 6th July 2020 (Figure 2, with estimates for other countries shown in Figure S2). Typically, the estimated peak of symptomatic cases in these countries ranged from 1.4 times (Chile) to 17.8 times larger (France) than the peak in the reported case data (Table 1). Moreover, in the five countries of these ten that had a clear initial peak before the end of May 2020, we estimated that the post-peak decline in the number of infections was steeper than that implied by the confirmed case curves (Figure 2B).

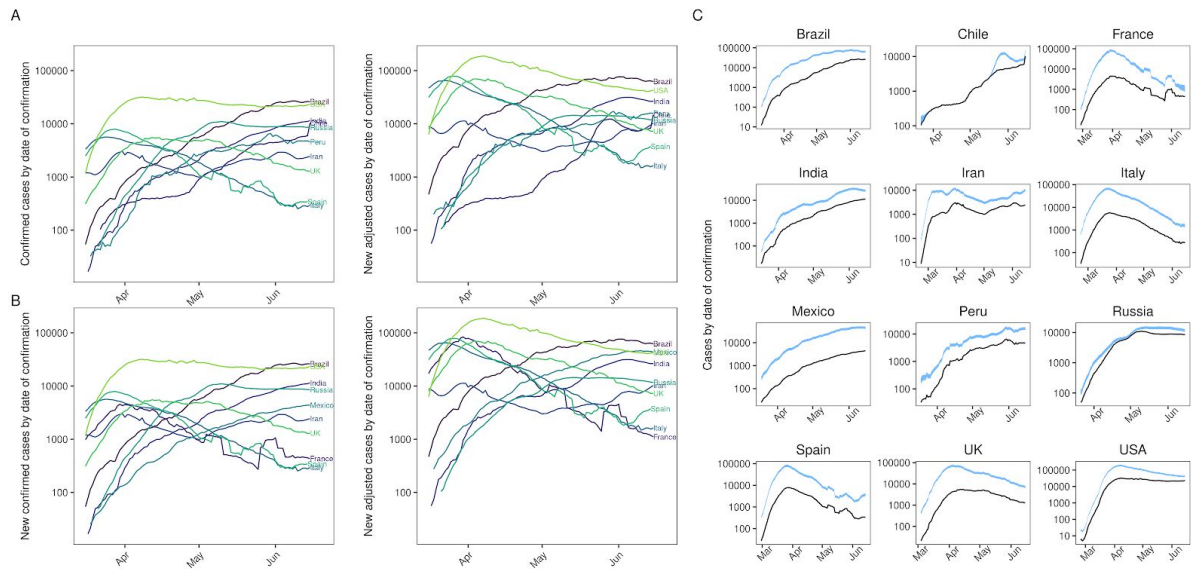


**Figure 2: Confirmed case curves adjusted for temporal under-ascertainment. Panel A: Confirmed cases (left) and adjusted cases (right) for the ten countries with the highest number of confirmed cases. Panel B: Confirmed cases (left) and adjusted cases (right) for the ten countries with the highest number of confirmed cases after adjusting for under-ascertainment. There are two countries which change between panels A and B: France and Mexico are replaced by Chile and Peru respectively. Panel C: The same curves plotted in panel A, but with a plot per country. Blue shaded region corresponds to the 95% CrI of the adjusted curves. Panels A and B highlight between country variation whereas panel C highlights within country variation.**

We also compared the estimated proportion of individuals infected in our model with seroprevalence studies that measured the prevalence of SARS-CoV-2 antibodies. We represent our cumulative incidence estimates in the same form as the observed serological estimates, as a percentage of the population. This is either the population of the country or the population of some smaller region or sub-region, depending on the serological dataset. We found that all but one of the published seroprevalence estimates fell within the 95% credible interval (CrI) of our estimated cumulative incidence curves over time, with the one exception being Denmark where we underestimated the observed seroprevalence (Figure 3).

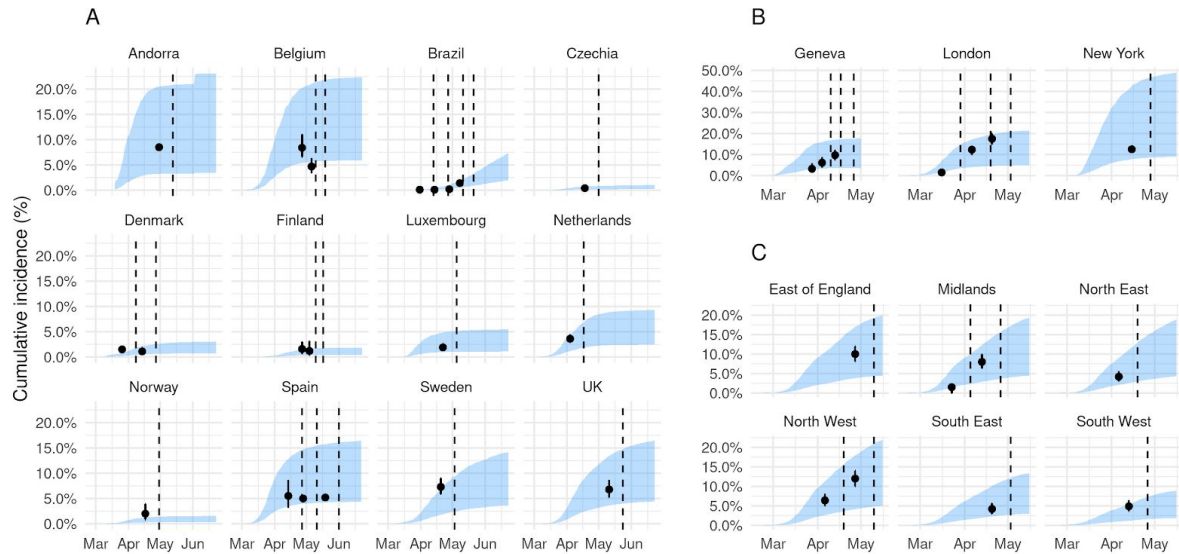


**Figure 3: Estimated infection prevalence curves compared with observed seroprevalence data.** Panel A: country-level comparisons. Panel B: City-level comparisons for Geneva, London and New York. Panel C: Regional-level comparisons, using six of the eight regions of England. North West and Yorkshire are aggregated together and London is shown above in Panel B: After adjusting the reconstructed new cases per day curves for potential asymptomatic infections and for the delay between onset of symptoms and confirmation, we sum up the cases and divide by the population in each country or region, to estimate the total percentage infected. We are then able to directly compare the model estimates to existing seroprevalence results (black points, with 95% binomial CI above and below). Dashed line shows the end of the serological testing period, therefore we lag the seroprevalence estimate by the mean delay between infection-to-seroconversion, which is likely to be around 14 days (21).

Applying our estimation method to all countries for which case and death time series data are available, we produced a map of seroprevalence estimates as of 16th June (Figure 4A), suggesting that most infections by this point had been concentrated in Europe and the US. We estimate that between 0.02% - 15% of populations in Europe have been infected. Cases have been rising in Latin America and Africa. For both continents combined, we estimate that between 0.00% - 3.48% of the population of these two continents had been infected as of 16 June 2020. We also reconstructed the early progression of the COVID-19 pandemic across Europe (Figure 4B), finding that the estimated infection prevalence over time was an order of magnitude higher than the confirmed case numbers suggest, with prevalence growing rapidly in late February and early March in several countries.



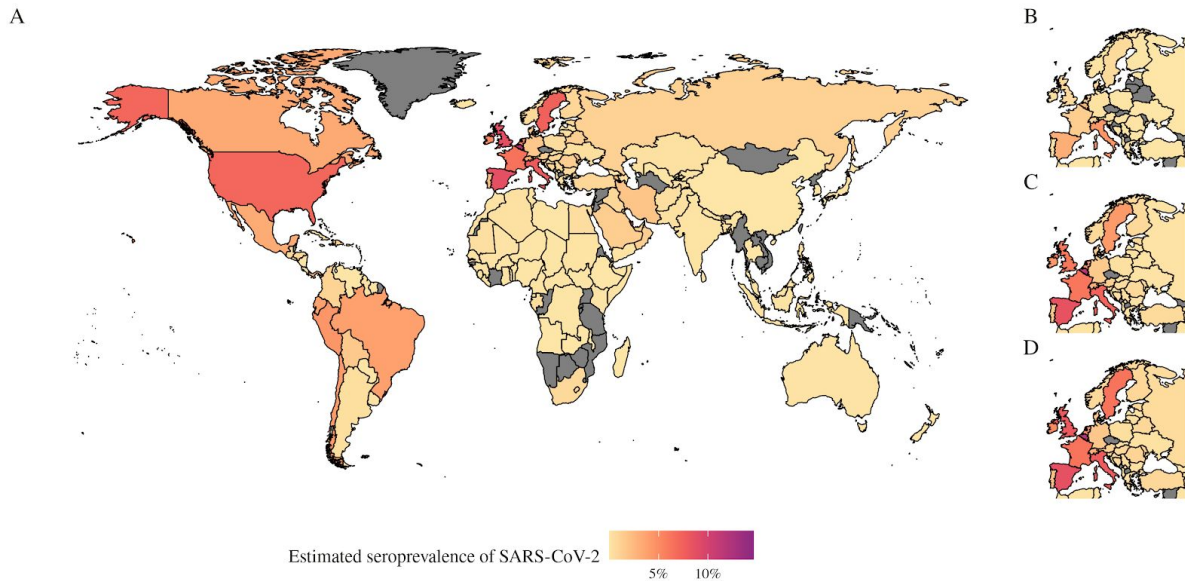


**Figure 4: Map of estimated seroprevalence in different countries over time. A) Estimated seroprevalence of SARS-CoV-2 globally as of 7th June 2020, for all countries we have estimates for. B–D) The estimated seroprevalence of SARS-Cov-2 in Europe on B) 31st March, C) 30th April and D) 31st May.**

## **Discussion**

The epidemiological and clinical characteristics of SARS-CoV-2 mean that a large proportion of infections may go undetected (14,22). In the absence of serological data, the ratio between cases and deaths, adjusted for delays from confirmation-to-outcome, can be used to derive estimates of the proportion of symptomatic cases reported. Using this approach, we estimated that case ascertainment dropped substantially in many countries during the peak of their first epidemic wave. Although serological surveys are beginning to emerge (22), many countries do not have such data available, or may only have results from a single cross-sectional survey. The methods and estimates presented here can therefore provide an ongoing picture of the underlying epidemics, including local level dynamics as fine-scale surveillance data become available (23,24).

Our analysis has some limitations. We assumed the age-adjusted baseline CFR was 1.4% (95% CrI: 1.2% - 1.5%) (4), which is broadly consistent with other published estimates (5,25,26), and we assumed a range of 10% - 70% of infections were asymptomatic (22,27–29) with a mean value of 50% (13). Given the uncertainty in these estimates, we propagated the variance in baseline CFR and range in proportion asymptomatic in the inference process so the final 95% credible interval reported for under-ascertainment reflects underlying uncertainty in the model parameters. We also assumed that deaths from COVID-19 are accurately reported. If local testing capacity is limited, or if testing policy affects attribution of deaths (for example, the evidence for the efficacy of post-mortem swabbing is lacking), deaths can be misattributed to a cause other than COVID-19. In that case, our model may underestimate the true burden of infection. Additionally, if a large proportion of transmission is concentrated within specific age groups, the effective CFR may be higher or lower than the assumed baseline; with better age-stratified temporal data on cases and deaths, it would be possible to explore the effect of this in more detail. However, our estimates were in general consistent

with published serological data, where available. Further, given that our estimates of under-ascertainment in many countries suggest that the numbers of symptomatic infections at the peak of the outbreak were one or two orders of magnitude larger than reported cases, even if deaths are under-reported, our estimates are still likely to be much closer to the true burden than locally reported cases imply. Our estimates of under-ascertainment over time require a time-series of COVID-19 deaths as an input, a data source that may also exhibit reporting variation. One notable example of this was Spain during June 2020 (Figure S1). However, as our Gaussian process model quantifies time-varying case ascertainment, it is able to account for positive or negative spikes in reporting (14) (see the Extended Methods section in the Supplementary Material for more details).

Since the temporal trend in under-ascertainment does not necessarily reflect trends in reported cases or testing effort, evidence synthesis methods such as the one presented here can provide additional insights into whether observed case patterns reflect the underlying epidemic dynamics. In the early stages of outbreaks, this method can provide an indication of whether a large proportion of cases are being detected – and hence whether transmission may be containable with targeted measures such as isolation and contact tracing – or whether transmission is more widespread and a more extensive response is required. Such estimates can also provide insights in the later stages of an outbreak, as they can indicate high levels of detection in countries that have achieved control. For example, in Australia, an adapted version of our model estimated that 80% (95% CrI: 55% - 100%) of cases had likely been ascertained during the outbreak (24). By adjusting for under-ascertainment, it is also possible to reconstruct the temporal dynamics of SARS-CoV-2 internationally. During February and early March 2020, importations of SARS-CoV-2 into the UK came primarily from Italy, Spain and France (30). This is consistent with the inferred progression of infection during this period in our model; we estimated that Italy, Spain, France and Belgium all had over 6.5% of the population infected by 31st March 2020 (30).

Consistent with other studies (3,22), we estimated that the true numbers of symptomatic cases and infections are appreciably larger than the number of confirmed cases reported (Figures 1 and 2). We also estimated that the timing of the peak level of symptomatic cases may be considerably earlier or later than the raw confirmed case curve suggests (Table 1). Accurate surveillance of an ongoing outbreak is crucial for estimating key epidemiological values such as the reproduction number, and hence evaluating the impact of control measures (21). If reported case numbers do not reflect the shape and magnitude of the underlying epidemic, it may bias estimates of transmission potential and effectiveness of interventions. If levels of under-ascertainment are increasing, early interventions may appear to be more effective than they actually are, which could lead to delays in imposing more stringent measures. Likewise, if ascertainment increases in the declining phase of an epidemic, the effectiveness of interventions may be underestimated, potentially leading to measures remaining in place for longer than they would have been had more accurate data been available.

## **Declarations**

### **Ethics approval and consent to participate**

Not applicable

### **Consent for publication**

Not applicable

### **Availability of data and materials**

The data we use is publicly available online from the European Centre for Disease Control (ECDC) (20). The code for the dCFR and under-reporting estimation model can be found here:

[https://github.com/thimotei/CFR\\_calculation](https://github.com/thimotei/CFR_calculation). The code to read in the under-ascertainment data and to reproduce the figures in this analysis can be found here:

[https://github.com/thimotei/covid\\_underreporting](https://github.com/thimotei/covid_underreporting).

### **Competing interests**

The authors declare that they have no competing interests

### **Funding**

The following funding sources are acknowledged as providing funding for the named authors. This research was partly funded by the Bill & Melinda Gates Foundation (INV-003174: YL).

DFID/Wellcome Trust (Epidemic Preparedness Coronavirus research programme 221303/Z/20/Z: KvZ). Elrha R2HC/UK DFID/Wellcome Trust/This research was partly funded by the National Institute for Health Research (NIHR) using UK aid from the UK Government to support global health research. The views expressed in this publication are those of the author(s) and not necessarily those of the NIHR or the UK Department of Health and Social Care (KvZ). This project has received funding from the European Union's Horizon 2020 research and innovation programme - project EpiPose (101003688: WJE, YL). This research was partly funded by the Global Challenges Research Fund (GCRF) project 'RECAP' managed through RCUK and ESRC (ES/P010873/1: CIJ). HDR UK (MR/S003975/1: RME). NIHR (16/137/109: YL). UK DHSC/UK Aid/NIHR (ITCRZ 03010: HPG). UK MRC (MC\_PC\_19065: RME, WJE, YL). Wellcome Trust (206250/Z/17/Z: AJK, TWR; 210758/Z/18/Z: JH, SA). NG was partially funded by an ARC DECRA fellowship (DE180100635)

The following funding sources are acknowledged as providing funding for the working group authors. Alan Turing Institute (AE). BBSRC LIDP (BB/M009513/1: DS). This research was partly funded by the Bill & Melinda Gates Foundation (INV-001754: MQ; INV-003174: KP, MJ; NTD Modelling Consortium OPP1184344: CABP, GM; OPP1180644: SRP; OPP1183986: ESN; OPP1191821: KO'R, MA). DFID/Wellcome Trust (Epidemic Preparedness Coronavirus research programme 221303/Z/20/Z: CABP). DTRA (HDTRA1-18-1-0051: JWR). ERC Starting Grant (#757688: CJVA, KEA; #757699: JCE, RMGJH; 757699: MQ). This project has received funding from the European Union's Horizon 2020 research and innovation programme - project EpiPose (101003688: KP, MJ, PK). This research was partly funded by the Global Challenges Research Fund (GCRF) project 'RECAP' managed through RCUK and ESRC (ES/P010873/1: AG, TJ). Nakajima Foundation (AE). This research was partly funded by the National Institute for Health Research (NIHR) using UK aid from the UK Government to support global health research. The views expressed in this publication are those of the author(s) and not necessarily those of the NIHR or the UK Department of Health and

Social Care (16/136/46: BJQ; 16/137/109: BJQ, CD, FYS, MJ; Health Protection Research Unit for Immunisation NIHR200929: NGD; Health Protection Research Unit for Modelling Methodology HPRU-2012-10096: TJ; NIHR200929: MJ; PR-OD-1017-20002: AR). Royal Society (Dorothy Hodgkin Fellowship: RL; RP\EA\180004: PK). UK MRC (LID DTP MR/N013638/1: GRGL, QJL; MC\_PC\_19065: AG, NGD, SC, TJ; MR/P014658/1: GMK). Authors of this research receive funding from UK Public Health Rapid Support Team funded by the United Kingdom Department of Health and Social Care (TJ). Wellcome Trust (206471/Z/17/Z: OJB; 208812/Z/17/Z: SC, SFlasche; 210758/Z/18/Z: JDM, KS, NIB, SFunk, SRM). No funding (AKD, AMF, DCT, SH).

### **Authors' contributions**

TWR and AJK conceived the study. TWK, AJK and NG developed the model and designed the inference framework. TWR wrote the initial draft manuscript with AJK. LW ran the model on a HPC and oversaw all computational aspects of the study. All authors read and made suggestions during the writing process.

### **Acknowledgements**

The following authors were part of the Centre for Mathematical Modelling of Infectious Disease 2019-nCoV working group. Each contributed in processing, cleaning and interpretation of data, interpreted findings, contributed to the manuscript, and approved the work for publication: Arminder K Deol, C Julian Villabona-Arenas, Thibaut Jombart, Carl A B Pearson, Kathleen O'Reilly, James D Munday, Sophie R Meakin, Rachel Lowe, Amy Gimma, Akira Endo, Emily S Nightingale, Graham Medley, Anna M Foss, Gwenan M Knight, Kiesha Prem, Stéphane Hué, Charlie Diamond, James W Rudge, Katherine E. Atkins, Megan Auzenberg, Stefan Flasche, Rein M G J Houben, Billy J Quilty, Petra Klepac, Matthew Quaife, Sebastian Funk, Quentin J Leclerc, Jon C Emery, Mark Jit, David Simons, Nikos I Bosse, Simon R Procter, Fiona Yueqian Sun, Samuel Clifford, Katharine Sherratt, Alicia Rosello, Nicholas G. Davies, Oliver Brady, Damien C Tully, Georgia R Gore-Langton.

## References

1. Hale T, Webster S, Petherick A, Phillips T, Kira B. Oxford COVID-19 Government Response Tracker [Internet]. Coronavirus Government Response Tracker. 2020. Available from: <https://www.bsg.ox.ac.uk/research/research-projects/coronavirus-government-response-tracker>
2. The effect of large-scale anti-contagion policies on the COVID-19 pandemic | Nature [Internet]. [cited 2020 Jun 16]. Available from: <https://www.nature.com/articles/s41586-020-2404-8>
3. Imperial College COVID-19 Response Team, Flaxman S, Mishra S, Gandy A, Unwin HJT, Mellan TA, et al. Estimating the effects of non-pharmaceutical interventions on COVID-19 in Europe. Nature [Internet]. 2020 Jun 8 [cited 2020 Jun 15]; Available from: <http://www.nature.com/articles/s41586-020-2405-7>
4. Davies NG, Kucharski AJ, Eggo RM, Gimma A, Edmunds WJ, Jombart T, et al. Effects of non-pharmaceutical interventions on COVID-19 cases, deaths, and demand for hospital services in the UK: a modelling study. Lancet Public Health [Internet]. 2020 Jun 2 [cited 2020 Jun 15]; Available from: <http://www.sciencedirect.com/science/article/pii/S246826672030133X>
5. Estimates of the severity of coronavirus disease 2019: a model-based analysis | Elsevier Enhanced Reader [Internet]. [cited 2020 Jun 14]. Available from: <https://reader.elsevier.com/reader/sd/pii/S1473309920302437?token=CD4A1F0ACB01423F61CEB8C44554DA6FB180FC86626AA572C31C95D75248AF38E3EE8719FC7866723A2F46A47F1B4BA1>
6. Hellewell J, Abbott S, Gimma A, Bosse NI, Jarvis CI, Russell TW, et al. Feasibility of controlling COVID-19 outbreaks by isolation of cases and contacts. Lancet Glob Health. 2020 Apr 1;8(4):e488–96.
7. Abbott et al. - 2020 - The transmissibility of novel Coronavirus in the e.pdf [Internet]. [cited 2020 Jun 15]. Available from: <https://www.ncbi.nlm.nih.gov/pmc/articles/PMC7156988.1/pdf/wellcomeopenres-5-17230.pdf>
8. Imperial College COVID-19 Response Team et al. - 2020 - Estimating the effects of non-pharmaceutical inter.pdf [Internet]. [cited 2020 Jun 13]. Available from: [https://www.nature.com/articles/s41586-020-2405-7\\_reference.pdf](https://www.nature.com/articles/s41586-020-2405-7_reference.pdf)
9. Early dynamics of transmission and control of COVID-19: a mathematical modelling study | Elsevier Enhanced Reader [Internet]. [cited 2020 Jun 15]. Available from: <https://reader.elsevier.com/reader/sd/pii/S1473309920301444?token=2B73274269CA34D33D1FF6FCCA2EB86350BDDA8FD11CAEA8EBDF3F7C40A186E75F59DA53A92251F919753BD0CD7D9B1E>
10. Lauer SA, Grantz KH, Bi Q, Jones FK, Zheng Q, Meredith HR, et al. The Incubation Period of Coronavirus Disease 2019 (COVID-19) From Publicly Reported Confirmed Cases: Estimation and Application. Ann Intern Med. 2020 May 5;172(9):577–82.
11. Tindale et al. - 2020 - Transmission interval estimates suggest pre-sympto.pdf [Internet]. [cited 2020 Jun 16]. Available from: <https://www.medrxiv.org/content/10.1101/2020.03.03.20029983v1.full.pdf>
12. Bai Y, Yao L, Wei T, Tian F, Jin D-Y, Chen L, et al. Presumed Asymptomatic Carrier Transmission of COVID-19. JAMA. 2020 Apr 14;323(14):1406–7.
13. Rivett L, Sridhar S, Sparkes D, Routledge M, Jones NK, Forrest S, et al. Screening of healthcare workers for SARS-CoV-2 highlights the role of asymptomatic carriage in COVID-19 transmission. van der Meer JW, editor. eLife. 2020 May 11;9:e58728.
14. Tsang TK, Wu P, Yun Lin YL, Lau E, Leung GM, Cowling BJ. Impact of changing case definitions for COVID-19 on the epidemic curve and transmission parameters in mainland China [Internet]. Epidemiology; 2020 Mar [cited 2020 Jun 16]. Available from: <http://medrxiv.org/lookup/doi/10.1101/2020.03.23.20041319>
15. Lourenco J, Paton R, Ghafari M, Kraemer M, Thompson C, Simmonds P, et al. Fundamental

- principles of epidemic spread highlight the immediate need for large-scale serological surveys to assess the stage of the SARS-CoV-2 epidemic [Internet]. *Epidemiology*; 2020 Mar [cited 2020 Jun 16]. Available from: <http://medrxiv.org/lookup/doi/10.1101/2020.03.24.20042291>
16. United Nations Population Division (2020). wpp2019: World Population Prospects 2019 [Internet]. (R package). Available from: <https://CRAN.R-project.org/package=wpp2019>
  17. Verity R, Okell LC, Dorigatti I, Winskill P, Whittaker C, Imai N, et al. Estimates of the severity of coronavirus disease 2019: a model-based analysis. *Lancet Infect Dis*. 2020 Jun 1;20(6):669–77.
  18. Roser M, Ritchie H, Ortiz-Ospina E, Hasell J. Coronavirus Pandemic (COVID-19) [Internet]. OurWorldInData.org. 2020. Available from: <https://ourworldindata.org/coronavirus>
  19. He X, Lau EHY, Wu P, Deng X, Wang J, Hao X, et al. Temporal dynamics in viral shedding and transmissibility of COVID-19. *Nat Med*. 2020 May;26(5):672–5.
  20. Download today's data on the geographic distribution of COVID-19 cases worldwide [Internet]. European Centre for Disease Prevention and Control. 2020 [cited 2020 Jun 15]. Available from: <https://www.ecdc.europa.eu/en/publications-data/download-todays-data-geographic-distribution-covid-19-cases-worldwide>
  21. Benny B, Amandine G, Kc P, Van S. Quantifying antibody kinetics and RNA shedding during early-phase SARS-CoV-2 infection. :20.
  22. Stringhini S, Wisniak A, Piumatti G, Azman AS, Lauer SA, Baysson H, et al. Seroprevalence of anti-SARS-CoV-2 IgG antibodies in Geneva, Switzerland (SEROCoV-POP): a population-based study. *The Lancet*. 2020 Jun;S0140673620313040.
  23. Galindo J. Faltan pruebas para medir el virus (y muchos casos por contar) en Latinoamérica. *El País* [Internet]. 2020 Apr 20 [cited 2020 Jul 7]; Available from: <https://elpais.com/sociedad/2020-04-20/faltan-pruebas-para-medir-el-virus-y-muchos-casos-por-contar-en-latinoamerica.html>
  24. Modelling the current impact of COVID-19 in Australia. :9.
  25. Russell TW, Hellewell J, Jarvis CI, van Zandvoort K, Abbott S, Ratnayake R, et al. Estimating the infection and case fatality ratio for coronavirus disease (COVID-19) using age-adjusted data from the outbreak on the Diamond Princess cruise ship, February 2020. *Eurosurveillance* [Internet]. 2020 Mar 26 [cited 2020 Jun 14];25(12). Available from: <https://www.eurosurveillance.org/content/10.2807/1560-7917.ES.2020.25.12.2000256>
  26. Shim E, Mizumoto K, Choi W, Chowell G. Estimating the Risk of COVID-19 Death During the Course of the Outbreak in Korea, February–May 2020. *J Clin Med*. 2020 Jun;9(6):1641.
  27. Mizumoto K, Kagaya K, Zarebski A, Chowell G. Estimating the asymptomatic proportion of coronavirus disease 2019 (COVID-19) cases on board the Diamond Princess cruise ship, Yokohama, Japan, 2020. *Eurosurveillance* [Internet]. 2020 Mar 12 [cited 2020 Jun 17];25(10). Available from: <https://www.eurosurveillance.org/content/10.2807/1560-7917.ES.2020.25.10.2000180>
  28. Emery JC, Russel TW, Liu Y, Hellewell J, Pearson CA, CMMID 2019-nCoV working group, et al. The contribution of asymptomatic SARS-CoV-2 infections to transmission - a model-based analysis of the Diamond Princess outbreak [Internet]. *Infectious Diseases (except HIV/AIDS)*; 2020 May [cited 2020 Jun 15]. Available from: <http://medrxiv.org/lookup/doi/10.1101/2020.05.07.20093849>
  29. Buitrago-Garcia DC, Egli-Gany D, Counotte MJ, Hossmann S, Imeri H, Ipekci AM, et al. The role of asymptomatic SARS-CoV-2 infections: rapid living systematic review and meta-analysis [Internet]. *Epidemiology*; 2020 Apr [cited 2020 Jun 17]. Available from: <http://medrxiv.org/lookup/doi/10.1101/2020.04.25.20079103>
  30. Preliminary analysis of SARS-CoV-2 importation & establishment of UK transmission lineages [Internet]. *Virological*. 2020 [cited 2020 Jun 16]. Available from: <https://virological.org/t/preliminary-analysis-of-sars-cov-2-importation-establishment-of-uk-transmission-lineages/507>

31. Linton NM, Kobayashi T, Yang Y, Hayashi K, Akhmetzhanov AR, Jung S, et al. Incubation Period and Other Epidemiological Characteristics of 2019 Novel Coronavirus Infections with Right Truncation: A Statistical Analysis of Publicly Available Case Data. *J Clin Med*. 2020 Feb;9(2):538.
32. Golding N. greta: simple and scalable statistical modelling in R. *J Open Source Softw*. 2019 Aug 12;4(40):1601.
33. Davies NG, Klepac P, Liu Y, Prem K, Jit M, Eggo RM. Age-dependent effects in the transmission and control of COVID-19 epidemics. *Nat Med*. 2020 Jun 16;1–7.
34. Iacobucci G. Covid-19: Care home deaths in England and Wales double in four weeks. *BMJ* [Internet]. 2020 Apr 22 [cited 2020 Jul 7];369. Available from: <https://www.bmj.com/content/369/bmj.m1612>
35. Gostic KM, McGough L, Baskerville E, Abbott S, Joshi K, Tedijanto C, et al. Practical considerations for measuring the effective reproductive number,  $R_t$ . :21.
36. Evaluating approaches to backcalculating cases counts by date of infection from cases counts by date of report [Internet]. Evaluating approaches to backcalculating cases counts by date of infection from cases counts by date of report. 2020. Available from: <https://github.com/epiforecasts/backcalc/blob/master/report.md>
37. European Centre for Disease Prevention and Control. Download today's data on the geographic distribution of COVID-19 cases worldwide [Internet]. Download today's data on the geographic distribution of COVID-19 cases worldwide. 2020. Available from: <https://www.ecdc.europa.eu/en/publications-data/download-todays-data-geographic-distribution-covid-19-cases-worldwide>

	Date		Value at peak	
Location	Peak of confirmed cases	Estimated change in peak date	New confirmed cases at peak	Estimated total cases (95% CrI)
Brazil	6th June 2020	0 days	54,771	122,512 (110,660 - 137,374)
Chile	18th June 2020	3 days	36,179	52,042 (47,828 - 56,338)
France	1st April 2020	0 days	7,578	134,594 (120,450 - 151,352)
India	21st June 2020	18 days	15,413	48,513 (43,433 - 54,939)
Iran	5th April 2020	0 days	5,275	17,931 (16,078 - 20,201)
Italy	22nd March 2020	0 days	6,557	75,521 (64,229 - 91,630)
Mexico	13th June 2020	0 days	5,222	55,661 (50,204 - 62,237)
Peru	4th June 2020	0 days	24,603	24,603 (22,121 - 27,629)
Russia	12th June 2020	4 days	11,656	15,604 (14,248 - 17,270)
Spain	27th March 2020	1 day	9,181	85,881 (77,697- 96,319)
UK	12th April 2020	0 days	8,719	100,870 (91,054 - 112,639)
USA	26th April 2020	21 days	48,529	280,631 (226,097 - 344,472)

**Table 1: Comparison between the confirmed and adjusted case numbers at their respective peaks for ten countries with the highest number of total confirmed cases and ten countries with the highest number of symptomatic cases after adjusting for under-ascertainment. Eight countries are in both lists, so the total is twelve distinct countries. We find that the peak of the case curves shifts when they are adjusted for under-ascertainment. Clearly, Mexico and Brazil haven't necessarily peaked yet, given that they are not as far along their epidemic as the other countries. Therefore, for these countries, we simply report the date and number of the highest number of cases to-date.**



## **Supplementary Material**

### **Extended Methods**

#### **Daily under-ascertainment calculation**

To calculate the level of under-ascertainment on a given day  $t$  in country  $c$ , first we estimate a delay-adjusted number of cases with outcomes known by time  $t$ ;  $dC_{c,t}$ . This delay-adjustment uses a discrete convolution correction method, accounting for all cases which to-date do not have known outcomes. Specifically, the correction term,  $dC_{c,t}$  for the proportion of cases with known outcomes on day  $t$  is given by

$$dC_{c,t} = \sum_{j=0}^t C_{c,t-j} g_j,$$

where  $C_{c,t}$ , the daily national case incidence and  $g_t$  the proportion of cases with known outcomes at time  $t$  after confirmation. Specifically,  $g_t$  represents the probability density function between confirmation-to-death, discretised between time-points using whichever time-resolution the data is on - typically days. We use a hospitalisation-to-death distribution approximated by a lognormal distribution with a mean of 13 days (8.7 - 20.9 days) and standard deviation of 12.7 days (6.4 - 26 days) (31) (see Table S3 for more details on this distribution and the other model parameters).

Let  $a_{c,t}$  denote the level of ascertainment at each time in each country. An estimator for the proportion of symptomatic cases ascertained on a given day is:

$$\hat{a}_{c,t} = \frac{\text{bCFR}}{d\text{CFR}_{c,t}},$$

where bCFR is the baseline case fatality ratio and  $d\text{CFR}_{c,t} = D_{c,t}/dC_{c,t}$  is the delay-adjusted case fatality ratio in that time and country, given by the ratio of daily deaths  $D_{c,t}$  to cases for which the outcome (death or survival) would be known by that time. However this point-wise estimator does not enable robust estimation of time-varying ascertainment rates.

#### **Fitting temporal trend with a Gaussian process**

ascertained cases and the apparent ascertainment rate  $a_{c,t}^*$ . I.e. the correction to the number of ascertained cases is applied in the model likelihood. We define the time-varying apparent ascertainment rates as:

$$\begin{aligned}\Phi^{-1}(a_{c,t}^*) &= f_c(t) + \epsilon_{c,t}, \\ \epsilon_{c,t} &\sim N(0, \sigma_{c,1}^2),\end{aligned}$$

where  $f_c(t)$  is a nonparametric function of time for country  $c$ ,  $\epsilon_{c,t}$  are independent daily noise terms, and  $\Phi^{-1}(x)$  is the inverse of the probit function, which maps function values to the unit interval - the

range of supported values of the ascertainment rate. We model  $f_c(t)$  as a realisation of a univariate zero-mean Gaussian process:

$$f_c(t) \sim \mathcal{GP}(\mathbf{0}, k(t, t'; \theta_c)),$$

with additive covariance function  $k(t, t'; \theta_c)$  given by the sum of two component covariance functions (implying summation of their resulting covariance matrices):  $k_{\text{bias}}$ , a ‘bias kernel’ modelling the average value of  $a_{c,t}$  over the whole period, and a squared exponential covariance function modelling temporal variation in ascertainment about that mean. These covariance functions are defined as:

$$\begin{aligned} k_{\text{bias}}(t, t') &= \sigma_{c,2}^2, \\ k_{SE}(t, t') &= \sigma_{c,3}^2 e^{-\frac{1}{2l_c^2} \|t-t'\|^2}. \end{aligned}$$

Note this summation of covariance functions is equivalent to defining  $f_c(t)$  as the sum of a single squared exponential covariance function and an intercept term with zero-mean normal prior with variance  $\sigma_{c,2}^2$ . Whilst this compositional Gaussian process representation is uncommon outside the Gaussian process machine-learning literature, it is computationally more convenient since it marginalises out an intercept parameter that would otherwise be poorly identified and lead to a correlated posterior density that would be difficult to sample from.

We consider that the Gaussian process represents the ‘signal’ in the apparent ascertainment rate; the true ascertainment rate  $a_{c,t}$ , and that the independent Gaussian error reflects noise in the apparent ascertainment rate over time, capturing extra-Poisson stochasticity (akin to a Poisson-lognormal model of overdispersion) in the time series of reported deaths, such as clustering of reporting of deaths. We therefore estimate the time varying ascertainment as:

$$\Phi^{-1}(a_{c,t}) = f_c(t)$$

We define the following prior distributions over the kernel and error parameters for each country:

$$\begin{aligned} \sigma_{c,1} &\sim N^+(0, 0.5^2) \\ \log(\sigma_{c,3}) &\sim N(1, 1^2) \\ \log(l_c) &\sim N(4, 0.5^2) \end{aligned}$$

where  $N^+(\cdot, \cdot)$  denotes a positive-truncated normal distribution, and we set the prior variance for the bias kernel (intercept term) to  $\sigma_{c,2} = 1$ .

### Choice of priors

The prior variance of 1 on the bias kernel (intercept term),  $k_{\text{bias}}(t, t') = \sigma_{c,2}^2$ , corresponds to a uniform prior on 0-1 for ascertainment holding the other components at zero (the probit link is the CDF of the standard normal, so a probit transformation of a standard normal yields a standard uniform distribution).

The half normal prior on the error variance,  $\epsilon_{c,t} \sim N(0, \sigma_{c,1}^2)$ , is a standard shrinkage prior that constrains the residual IID errors to 0, or small values in the absence of evidence to the contrary.

The lognormal prior on the GP amplitude parameter,  $\sigma_{c,3}^2$ , does not shrink towards zero, since that would imply a prior assumption that there is no temporal correlation. Similarly, we use a lognormal prior on the lengthscale parameter,  $l_c$ , since a prior mass close to zero implies very rapid changes in the ascertainment rate. The two lognormal priors were chosen manually to enable a wide range of ‘shapes’ of the ascertainment rate, without leading to long periods of ascertainment at the boundaries (close to 1 or zero, since the probit links squishes large positive/negative values toward those). I.e. they were chosen to be minimally informative.

Finally, we incorporate uncertainty around the assumed baseline CFR by treating it as a random variable with an informative prior. Specifically, we assume it is normally distributed with mean and SD matching the reported CIs (17), and truncated from 0% to 100%.

### **Numerical procedure**

We fit the model by Hamiltonian Monte Carlo using the R packages greta and greta.gp (32). Each model was fitted with 500 independent MCMC chains (a computationally-efficient strategy to yielding large numbers of posterior samples) of 10000 samples each, after discarding an initial 1000 samples per chain during a warm up period during which the sampler was tuned. Using these 500,000 posterior samples, we estimated the posterior median of the posterior and 95% credible interval (CrI) for each time point (black filled line for median and blue shaded region for 95% CrI in Figure 1 and Figure S1).

We assessed convergence of the chains using the Gelman–Rubin convergence diagnostic.

Specifically, we tested whether  $\hat{R} \leq 1.1$  and whether  $\min(n_{\text{eff}}) > 1000$  across all chains. Once these conditions were satisfied, we assumed convergence to the posterior.

### **Data**

The input data for the model is a time-series of new cases and new deaths. The temporal and spatial resolution of the input data directly reflects the resolution of the resulting estimates. I.e. if the input data corresponds to the new cases and new deaths each day for a country, then we are able to estimate the under-ascertainment each day for that country. The spatial resolution is important for the accuracy of the estimates, given that some countries have highly heterogeneous population distributions, with concentrated outbreaks in large cities. We therefore use regional data, where it is available for direct comparisons with seroprevalence data (Figure 3) in such countries. We typically find that the accuracy of the estimates increases as the spatial resolution of the input data increases. Unfortunately regional data is not as easy to find from a centralised and regularly updated source.

For the new cases and new deaths time-series data required as a model input, we use the publicly available data from the European Centre for Disease Control (found here:

<https://www.ecdc.europa.eu/en/publications-data/download-todays-data-geographic-distribution-covid>

[-19-cases-worldwide](#)), which is updated daily. Countries must have had at least ten deaths, for longer than ten days, for their estimates to be computed. Fewer deaths, or for a few days (or both) results in spurious estimates with 95% credible intervals that typically range from 0-100% of the cases ascertained.

### **Further details on methodology and limitations**

#### **Baseline CFR**

We assumed the age-adjusted baseline CFR is 1.4% (95% CrI: 1.2% - 1.5%) (4), which is broadly consistent with other published estimates (5,25,26), and assumed a range of 10% - 70% of infections were asymptomatic (22,27–29) with a mean value of 50% (13). Given the uncertainty in these estimates, we propagated the variance in baseline CFR and range in proportion asymptomatic in the inference process so the final 95% credible interval reported for under-ascertainment reflects underlying uncertainty in the model parameters. We also assumed that deaths from COVID-19 are accurately reported. If local testing capacity is limited, or if testing policy affects attribution of deaths (for example, the evidence for the efficacy of post-mortem swabbing is lacking), deaths can be misattributed to a cause other than COVID-19. In that case, our model may underestimate the true burden of infection. However, our estimates were consistent with published serological data. Given that our estimates of under-ascertainment in many countries suggest that the numbers of symptomatic infections at the peak of the outbreak were an order of magnitude larger than reported cases, even if deaths are under-reported, our estimates are still likely to be much closer to the true burden than locally reported cases imply. Our estimates of under-ascertainment over time require a time-series of COVID-19 deaths as an input, a data source that may also exhibit reporting variation. One significant example of this was Spain during June 2020 (Figure S1). However, as our Gaussian process model quantifies time-varying case ascertainment, it is able to account for positive or negative spikes in reporting (14). Specifically, we are able to infer what are known as the inducing points of the temporal trends: the most likely times trends in the under-ascertainment estimates change qualitatively (see the Extended Methods section in the Supplementary Material for more details on the model fitting procedure).

Assuming a fixed baseline CFR of 1.4% (95% CrI: 1.2% - 1.5%) means that we are not accounting for the differences in underlying age distributions between different countries. It is well-known that the severity of COVID-19 has a strong age-dependency (17). Therefore, it is likely that in countries with younger-skewed populations that we overestimate the ascertainment rate in such countries and vice versa in older-skewed countries. We have implemented an indirect age-adjusted baseline CFR for each country, but this comes with its own set of limitations. The main one being that the age-adjusted CFR results were able to be estimated as they assumed a flat attack rate across age-groups (17). In the absence of case and death time series input data stratified by age, we opted for the parsimonious method of a flat baseline CFR across all countries. To investigate the sensitivity of our methods to this flat CFR, we reproduced Figure 3 with the age-adjusted ascertainment estimates (Figure S7).

#### **Proportion of infections that are asymptomatic**

Adjusting for the true number of asymptomatic was performed by simply assuming a wide range, reflecting the still-present uncertainty in the literature of 10-70% of all infections. This proportion scales the adjusted case curves. The proportion of asymptomatic/pre-symptomatic infections has been estimated to also vary with age (33). Again, in the absence of age-stratified data globally, we opt for a

simple adjustment, which is equivalent across all settings. As more detailed data comes in, it would be possible to refine and improve the accuracy of the methods presented.

### **Reporting caveats including under-reporting of deaths**

We use data on reported deaths, but these values may represent different events across different countries. For example, some countries did not initially report deaths from care homes (34). There have also been instances of data being retrospectively updated, such as when Spain recorded a negative value of -1918 deaths on the 26th May. Our methods account for this temporal variation by considering the using the Gaussian process to represent the ‘signal’ in the apparent ascertainment rate, capturing extra-Poisson stochasticity (akin to a Poisson-lognormal model of overdispersion) in the time series of reported deaths, such as clustering of reporting of deaths (See subsection Fitting temporal trend with a Gaussian process for more details). However, the large spike in the Spanish data was outside the range of routine modelled day-to-day variation and so the resulting CrI of our estimates were inconsistent with observed dynamics. We therefore only ran inference on data up until the 26th May and did not include later dates. A more detailed analysis on the Spanish dataset could redistribute the large negative number of deaths to surrounding days, such that the model could deal with the negative deaths more accurately.

### **Time delay assumptions**

There are multiple time delays during the reporting process, from confirmation to hospitalisation to death (35). When estimating cumulative incidence within a country and presenting it as a percentage of the total population, we adjust the reported case curves for under-ascertainment and potential asymptomatic infections. In doing so, we are attempting to describe the number infected at point of infection rather than point of confirmation. To do so, we mean-shift the dates by the mean of the distribution between onset of symptoms and confirmation (ref). The distribution has a mean of 9 days (add uncertainty). Mean-shifting is a crude adjustment, with known errors. In doing so, we assume that reporting delays are static over-time and equivalent for all countries. Given that we are performing analysis globally, other more complex methods were not opted for as they would have incurred substantial computational costs on top of the computationally intensive Gaussian process framework. Further, between-country variation in delays until confirmation would need to be considered if a more detailed approach were taken, which would require more detailed data than is known to exist for most countries. However, as we only report infection time as cumulative incidence, a substantial portion of the individual variation in infection time would not be reflected in the incidence, as only the dates which truly occurred before the mean of the delay distribution would be incorrect (those occurring after the mean of the distribution would already be included in the cumulative count). More accurate estimation may be possible with good progress made attempting to solve imputing infection dates from date-of-confirmation data (36). Such methods were motivated by Gostic et al. (35) and are able to accurately reconstruct the true infection curves, validated against simulated data.

## Supplementary Figures

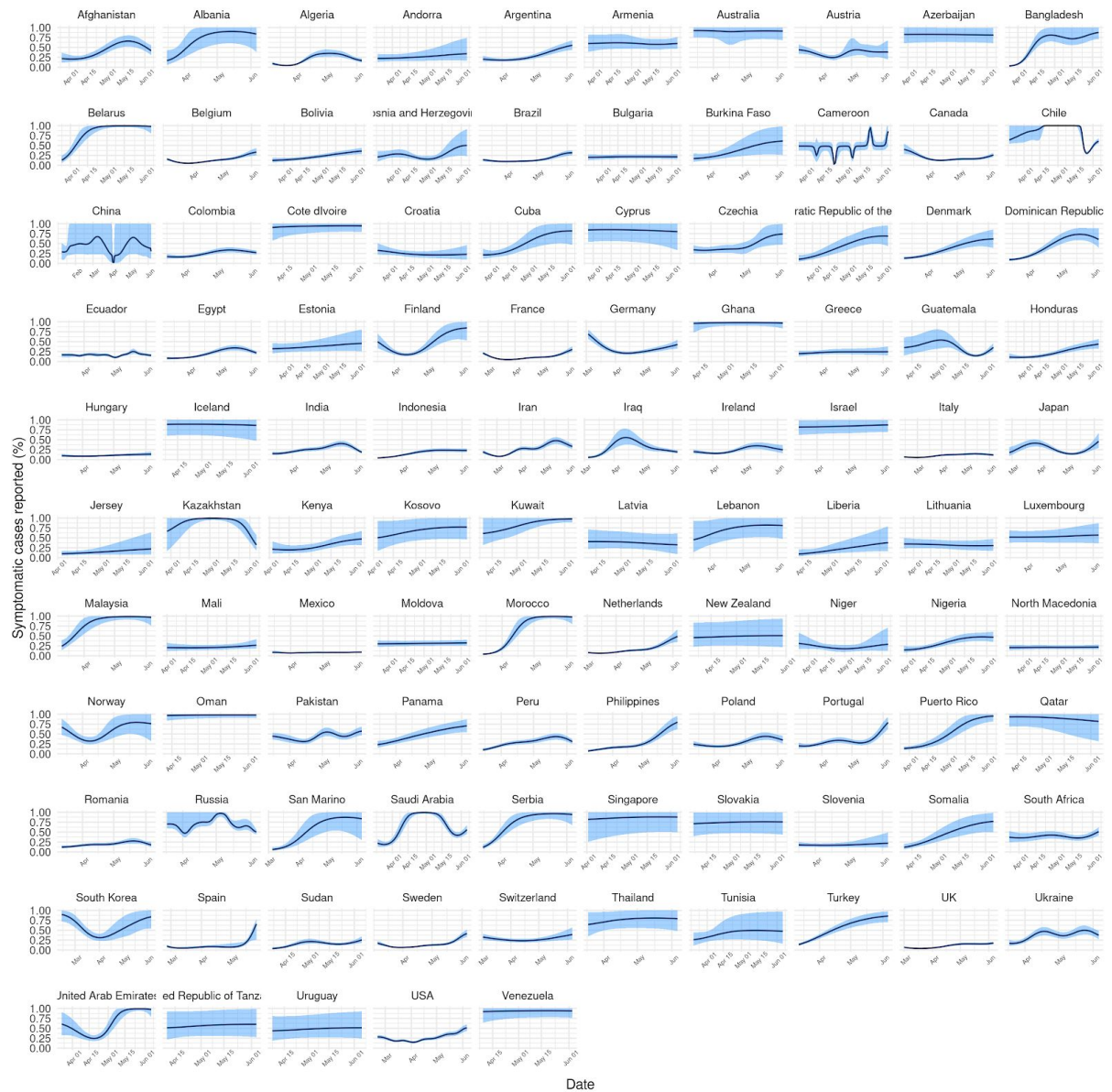


**Figure S1: Temporal variation in under-reporting for all countries with greater than 10 deaths for more than 50 days.**

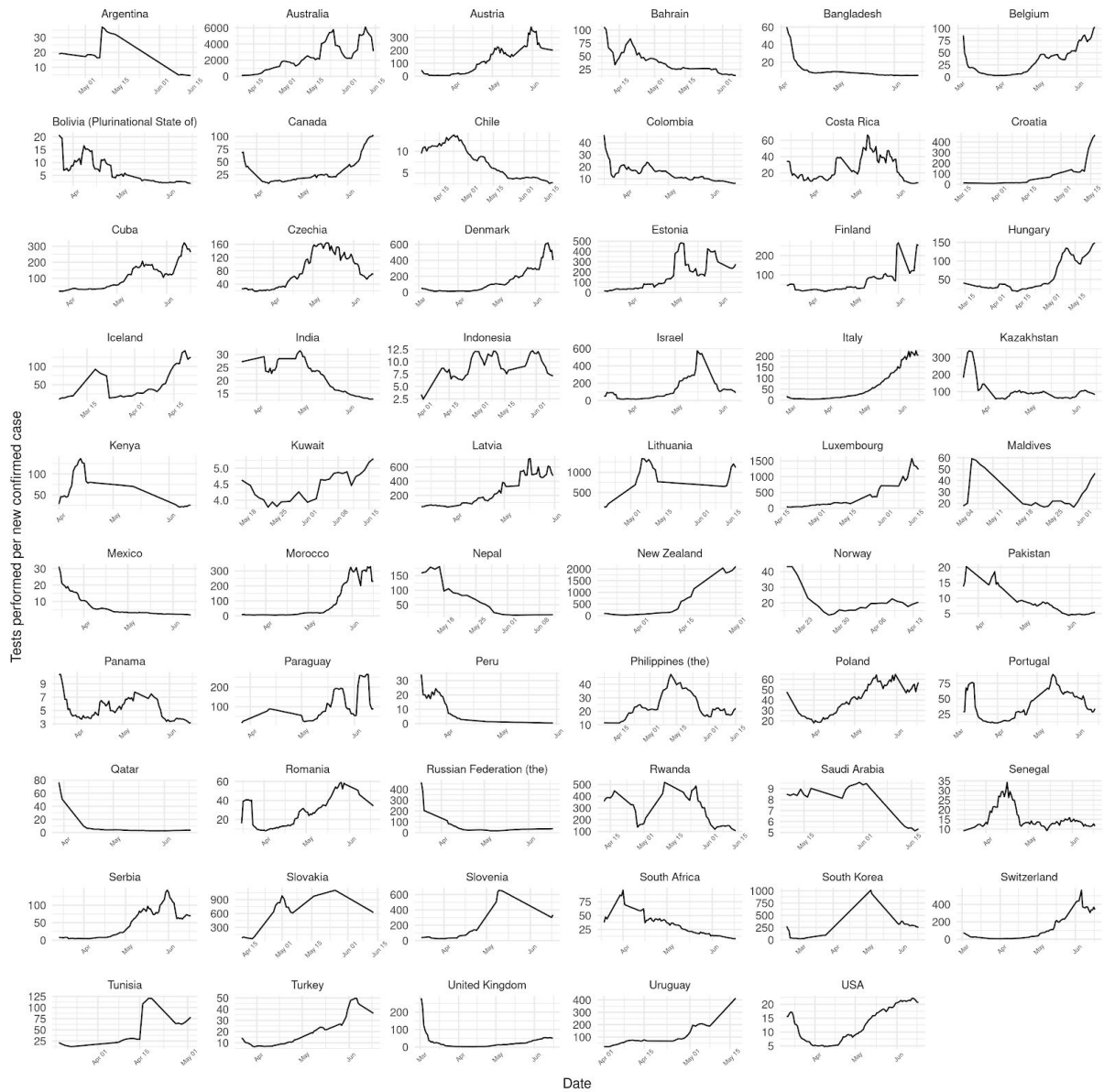


**Figure S2: Temporal variation in testing effort for all countries there was data for in the Our World In Data database (18).**

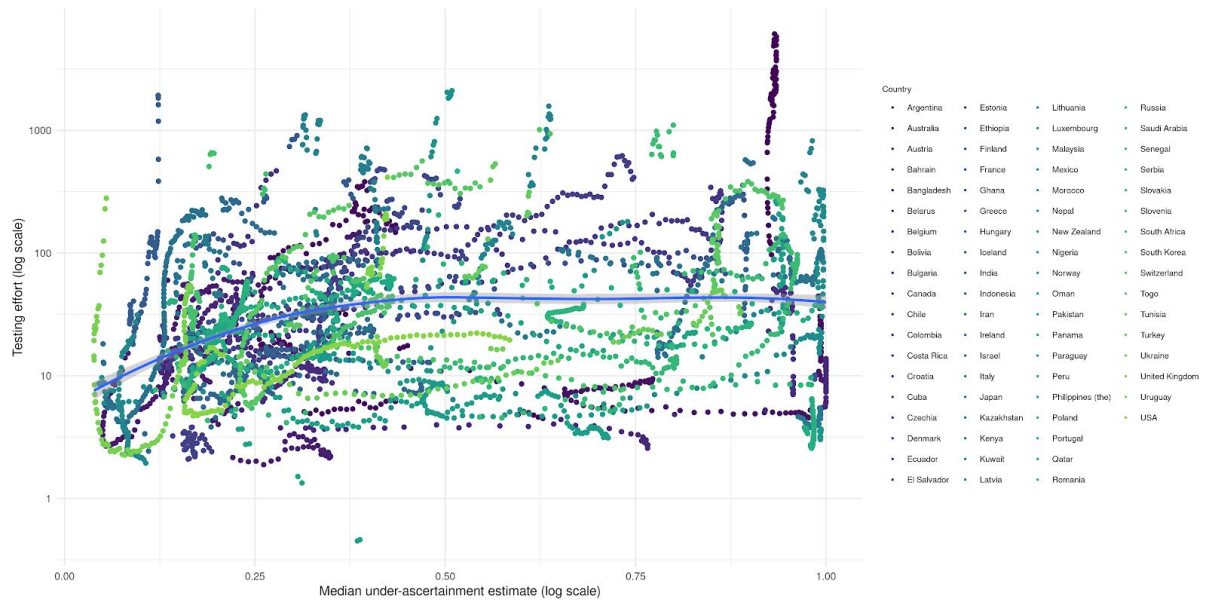


**Figure S3: the relationship between case ascertainment and testing effort.** We define testing effort as the 7-day moving average of the number of new tests per new cases each day. We plot the under-ascertainment estimates along with the testing effort estimates for all countries we have both data for. We then fit, using a loess curve to highlight the positive but weak relationship ( $\tau = 0.16$ , where  $\tau$  is Kendall's rank coefficient).



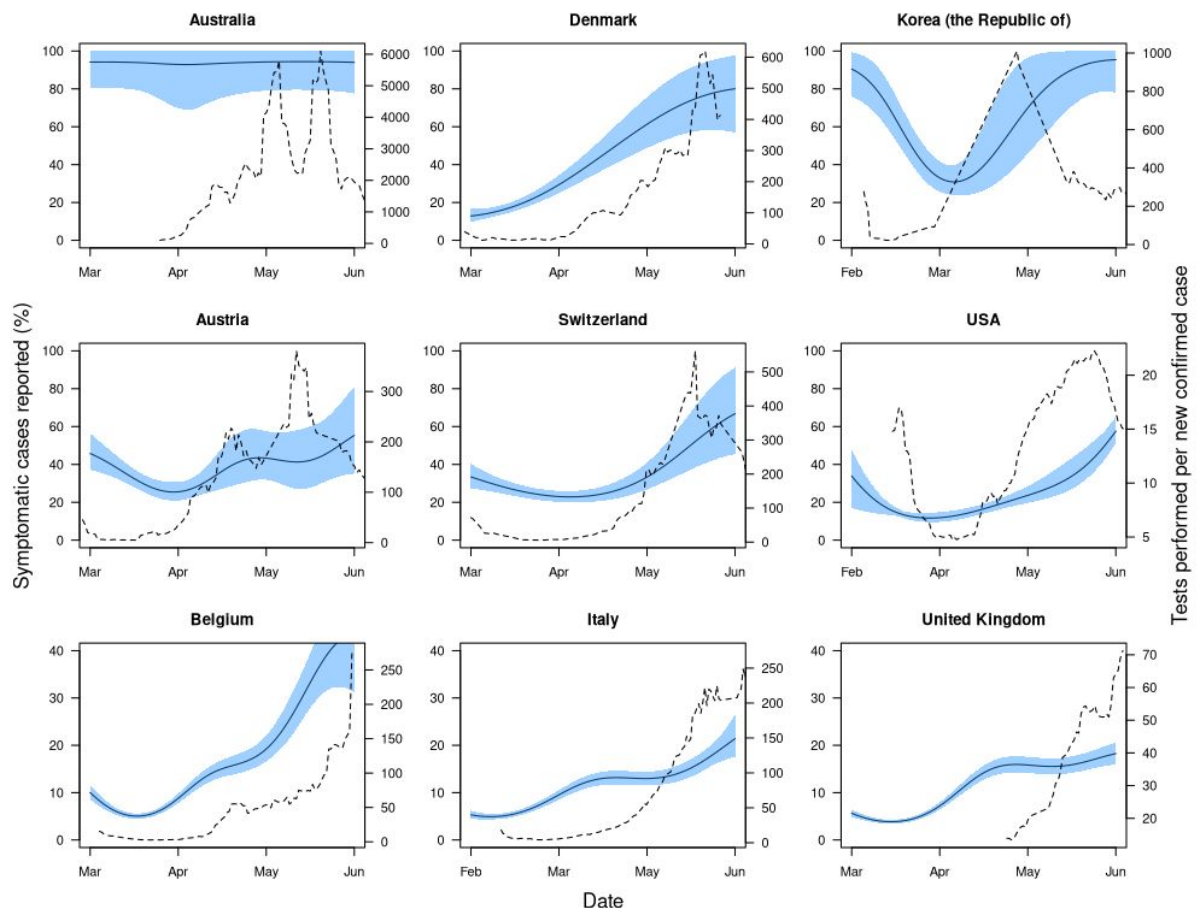


**Figure S4: Temporal variation in under-ascertainment and testing effort for the nine countries with the maximum total cases that we have reliable testing effort estimates for.** This figure differs from Figure 1 as the results are computed using the indirectly age-adjusted baseline CFR for each country.

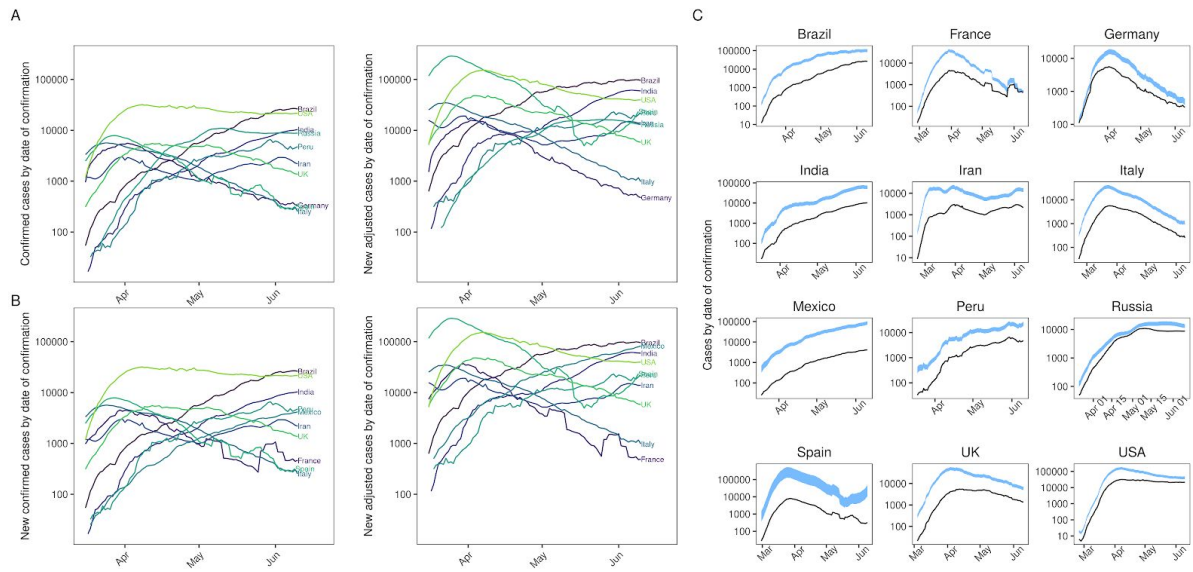


**Figure S5: Confirmed case curves adjusted for temporal under-ascertainment adjusted indirectly for age.** The results are similar to those in Figure 2 but have been computed using an indirectly age-adjusted baseline CFR for each country.

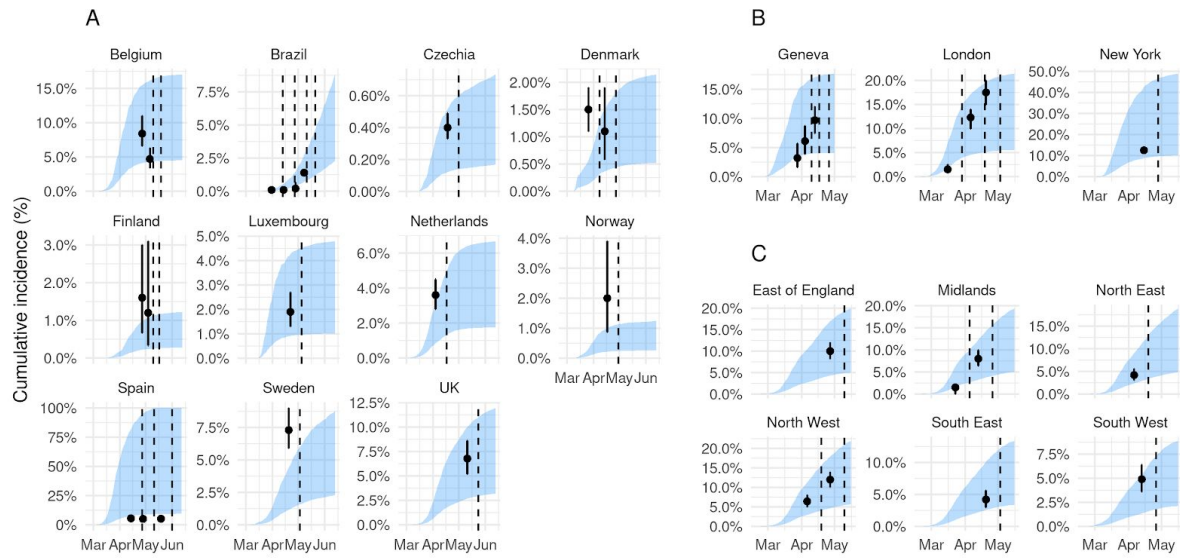


**Figure S6: Estimated infection prevalence curves compared with observed seroprevalence data.**  
The results are similar to those in Figure 3 but have been computed using an indirectly age-adjusted baseline CFR for each country.



**Figure S7: : Temporal variation in under-reporting for all countries with greater than 10 deaths for more than 50 days. The results are similar to those in Figure S1 but have been computed using an indirectly age-adjusted baseline CFR for each country.**

Country	Sampling end date	Percentage positive (95% CI)	Source
Andorra	13th May	8.5% (8.3% - 8.7%)	<a href="#">Martinez Benazet agraeix a institucions, voluntaris ia la població que ha participat en l'estudi nacional d'anticossos</a>
Belgium	10th May	8.4% (6.6% - 11%)	<a href="#">COVID-19 – WEKELIJKS EPIDEMIOLOGISCH BULLETIN VAN 29 MEI 2020 INHOUDSTAFEL</a>
Belgium	19th May	4.7% (3.4% - 6.3%)	<a href="#">COVID-19 – WEKELIJKS EPIDEMIOLOGISCH BULLETIN VAN 29 MEI 2020 INHOUDSTAFEL</a>
Brazil	13th Apr	0.1% (0.01% - 0.17%)	<a href="#">Apresentação do PowerPoint</a>
Brazil	27th Apr	0.1% (0.05% - 0.29%)	<a href="#">Apresentação do PowerPoint</a>
Brazil	11th May	0.2% (0.27% - 0.69%)	<a href="#">Apresentação do PowerPoint</a>
Brazil	21st May	1.4% (1.2% - 1.5%)	<a href="#">Remarkable variability in SARS-CoV-2 antibodies across Brazilian regions: nationwide serological household survey in 27 states</a>
Czech Republic	1st May	0.4% (0.33% - 0.49%)	<a href="https://koronavirus.mzcr.cz/infekce-covid-19-prosla-ceskou-populaci-v-elmi-mirne-podobne-jako-v-okolnich-zemich/">https://koronavirus.mzcr.cz/infekce-covid-19-prosla-ceskou-populaci-v-elmi-mirne-podobne-jako-v-okolnich-zemich/</a>
Denmark	8th Apr	1.5% (1.1% - 1.9%)	<a href="#">Estimation of SARS-CoV-2 infection fatality rate by real-time antibody screening of blood donors</a>
Denmark	27th Apr	1.1% (0.58% - 1.9%)	<a href="#">Notat: Foreløbige resultater fra den repræsentative seroprævalensundersøgelse af COVID-19. Den 20. maj 2020</a>
Finland	10th May	1.6% (0.67% - 3.0%)	<a href="#">Koronaepidemiaan väestöserologiatutkimuksen viikkoraportti</a>
Finland	17th May	1.2% (0.33% - 3.1%)	<a href="#">Koronaepidemiaan väestöserologiatutkimuksen viikkoraportti</a>
Luxembourg	5th May	1.9% (1.3% - 2.7%)	<a href="#">Prevalence of SARS-CoV-2 infection in the Luxembourgish population: the CON-VINCE study.</a>
Netherlands	17th Apr	3.6% (2.8% - 4.5%)	<a href="#">Children and COVID-19</a>
Norway	30th Apr	2% 0.87% - 3.9%)	<a href="#">Truleg berre ein liten andel som har vore smitta av koronavirus i Noreg</a>
Spain	27 Apr	5.5% (3.2% - 8.6%)	<a href="#">Primer estudi que revela la protecció de la nostra població davant del coronavirus</a>
Spain	11 May	5% (4.8% - 5.2%)	<a href="#">Consumo y Bienestar Social - Gabinete de Prensa - Notas de Prensa</a>
Spain	1 Jun	5.2% (5.0% - 5.4%)	<a href="#">ESTUDIO ENE-COVID19: SEGUNDA RONDA</a>
Sweden	3 May	7.3% (5.9% - 9.0%)	<a href="#">Första resultaten från pågående undersökning av antikroppar för covid-19-virus</a>
UK	24 May	6.78% (5.2% - 8.6%)	<a href="#">Coronavirus (COVID-19) Infection Survey pilot</a>

**Table S1: A summary of the country-level serological studies we used for comparison against our model estimates.**

Country	City or region	Sampling end date	Percentage positive (95% CI)	Source
UK	East of England	2020-05-10	10% (8.2% - 12%)	<a href="#">Sero-surveillance of COVID-19 - GOV.UK</a>
UK	London	2020-03-29	1.5% (0.84% - 2.5%)	<a href="#">Sero-surveillance of COVID-19 - GOV.UK</a>
UK	London	2020-04-19	12.3% (10% - 14%)	<a href="#">Sero-surveillance of COVID-19 - GOV.UK</a>
UK	London	2020-05-03	17.5% (15% - 20%)	<a href="#">Sero-surveillance of COVID-19 - GOV.UK</a>
UK	Midlands	2020-04-05	1.5% (0.02% - 0.72%)	<a href="#">Sero-surveillance of COVID-19 - GOV.UK</a>
UK	Midlands	2020-04-26	8% (6.4% - 9.9%)	<a href="#">Sero-surveillance of COVID-19 - GOV.UK</a>
UK	North East	2020-04-19	4.2% (3.0% - 5.6%)	<a href="#">Sero-surveillance of COVID-19 - GOV.UK</a>
UK	North West	2020-05-10	12% (10% - 14%)	<a href="#">Sero-surveillance of COVID-19 - GOV.UK</a>
UK	North West	2020-04-19	6.4% (5.0% - 8.1%)	<a href="#">Sero-surveillance of COVID-19 - GOV.UK</a>
UK	South East	2020-05-03	4.2% (3.0% - 5.6%)	<a href="#">Sero-surveillance of COVID-19 - GOV.UK</a>
UK	South West	2020-04-26	4.9% (3.6% - 6.4%)	<a href="#">Sero-surveillance of COVID-19 - GOV.UK</a>
Switzerland	Geneva	2020-04-10	3.2% (1.6% - 5.7%)	<a href="#">Repeated seroprevalence of anti-SARS-CoV-2 IgG antibodies in a population-based sample from Geneva, Switzerland</a>
Switzerland	Geneva	2020-04-17	6.1% (3.9% - 8.7%)	<a href="https://www.medrxiv.org/content/10.1101/2020.05.02.20088898v1.full.pdf">https://www.medrxiv.org/content/10.1101/2020.05.02.20088898v1.full.pdf</a>
Switzerland	Geneva	2020-04-26	9.7% (7.4% - 12%)	<a href="#">Repeated seroprevalence of anti-SARS-CoV-2 IgG antibodies in a population-based sample from Geneva, Switzerland</a>
USA	New York State	2020-04-28	12.5% (12% - 13%)	<a href="#">Cumulative incidence and diagnosis of SARS-CoV-2 infection in New York</a>

**Table S2: A summary of the city-level or regional-level serological studies we used for comparison against our model estimates.**

Parameter	Description	Value (95% CI or CrI if applicable) or prior specification	Literature source (if applicable)
$c_t$	Number of new cases on day $t$	N/A	<a href="#">ECDC website</a> (37)
$d_t$	Number of new deaths on day $t$	N/A	<a href="#">ECDC website</a> (37)
$\hat{a}_{c,t}$	The proportion of cases ascertained on day $t$	N/A	N/A
$f_t$	Discretised probability density of death on day $t$	Mean: 13 days (8.7 - 20.9) SD: 12.7 days (6.4 - 21.8)	Linton et al. (2020) (31)
bCFR	The assumed baseline CFR	1.4% (1.2% - 1.5%)	Verity et al. (2020) (17)
dCFR $_{c,t}$	The country specific delay-adjusted CFR	N/A	N/A
$\sigma_{c,2}^2$	Bias term in kernel of GP	$\sigma_{c,2}^2 \sim \text{Uniform}(0, 1)$	N/A
$\epsilon_{c,t}$	Error variance term in GP	$\epsilon_{c,t} \sim N(0, \sigma_{c,1}^2)$	N/A
$\sigma_{c,3}^2$	GP amplitude parameter	$\log(\sigma_{c,3}) \sim N(1, 1^2)$	N/A
$l_c$	Lengthscale parameter	$\log(l_c) \sim N(4, 0.5^2)$	N/A

**Table S3: A summary of the parameters, distributions and output quantities either as inputs or outputs of our under-ascertainment model**